Biogeosciences Discuss., 9, 11815–11842, 2012
www.biogeosciences-discuss.net/9/11815/2012/
doi:10.5194/bgd-9-11815-2012

Biogeosciences Discussions

Detection of large above ground biomass variability in lowland forest ecosystems by airborne LiDAR

J. Jubanski[1], U. Ballhorn[1,2], K. Kronseder[1,2], J. Franke[1], and F. Siegert[1,2]

[1]Remote Sensing Solutions GmbH, Isarstrasse 3, 82065 Baierbrunn, Germany
[2]Biology Department II, GeoBio Center, Ludwig-Maximilians-University, Grosshaderner Strasse 2, 82152 Planegg-Martinsried, Germany

Received: 1 August 2012 – Accepted: 15 August 2012 – Published: 31 August 2012

Correspondence to: J. Jubanski (jubanski@rssgmbh.de)

Published by Copernicus Publications on behalf of the European Geosciences Union.

Abstract

Quantification of tropical forest Above Ground Biomass (AGB) over large areas as input for Reduced Emissions from Deforestation and forest Degradation (REDD+) projects and climate change models is challenging. This is the first study which attempts to estimate AGB and its variability across large areas of tropical lowland forests in Central Kalimantan (Indonesia) through correlating airborne Light Detection and Ranging (LiDAR) to forest inventory data. Two LiDAR height metrics were analysed and regression models could be improved through the use of LiDAR point densities as input ($R^2 = 0.88$; $n = 52$). Surveying with a LiDAR point density per square meter of 2–4 resulted in the best cost-benefit ratio. We estimated AGB for 600 km of LiDAR tracks and showed that there exists a considerable variability of up to 140 % within the same forest type due to varying environmental conditions. Impact from logging operations and the associated AGB losses dating back more than 10 yr could be assessed by LiDAR but not by multispectral satellite imagery. Comparison with a Landsat classification for a 1 million ha study area where AGB values were based on site specific field inventory data, regional literature estimates, and default values by the Intergovernmental Panel on Climate Change (IPCC) showed an overestimation of 46 %, 102 %, and 137 %, respectively. The results show that AGB overestimation may lead to wrong GHG emission estimates due to deforestation in climate models. For REDD+ projects this leads to inaccurate carbon stock estimates and consequently to significantly wrong REDD+ based compensation payments.

1 Introduction

In 2008 worldwide deforestation and forest degradation emissions are estimated to account for about 6–17 % of the total anthropogenic carbon dioxide (CO_2) emissions (Van der Werf et al., 2009). In the period of 1990 to 2005 annually about 13 million ha of tropical forest were deforested and with 0.98 % South and Southeast Asia had one

BGD
9, 11815–11842, 2012

of the highest annual deforestation rates between 2000 and 2005 (FAO, 2006). Human economic activities such as the establishment of industrial timber estates and large-scale oil palm plantations, legal and illegal logging, and shifting cultivation are the main drivers for deforestation and forest degradation in this region (Hansen et al., 2009; Langner et al., 2007; Langner and Siegert, 2009; Rieley and Page, 2005; Siegert et al., 2001). One important measure of the United Nations Framework Convention on Climate Change (UNFCCC) to curb Green House Gas (GHG) emissions from this sector is the Reduced Emissions from Deforestation and forest Degradation (REDD+) programme. Implementation of REDD+ projects depend on accurate estimates of GHG emissions avoided, because inaccurate estimates can lead to carbon credits that are not covered by the specific REDD+ project. Typically in tropical forests the main carbon pool is the Above Ground Biomass (AGB) (Gibbs et al., 2007; FAO, 1997; Chave et al., 2005). To estimate CO_2 emissions from deforestation and forest degradation the change in AGB corresponding to information on both the area of forest loss and/or the level of degradation is needed, which remains a considerable challenge in tropical forests. Especially AGB loss and the associated CO_2 emissions from forest degradation by logging and fire are difficult to assess and monitor because their impacts may vary significantly. Detection of degradation is also important as it is predicted that degraded and regrowing forests will include increasingly large areas of the tropical regions (Gibbs et al., 2007). The most accurate method of AGB estimation is based on forest inventories where field measurements are extrapolated to AGB values through allometric equations (FAO, 1997; Chave et al., 2005). Although this approach provides precise AGB estimations the biotic and structural complexity of tropical ecosystems make forest inventories difficult, time-consuming, and expensive: generic relationships may not fit to specific areas, growth conditions may vary greatly within a specific forest ecosystem, and to produce regionally and globally consistent results is challenging (Gibbs et al., 2007; Chave et al., 2005). Further there is considerable uncertainty about the spatial variability of AGB in different tropical forest types and the impact of logging and fire on AGB stock. AGB can also be estimated by remote sensing technologies,

BGD
9, 11815–11842, 2012

but no such instrument can measure AGB directly, therefore in situ data collection is always inevitably (Drake et al., 2003; Rosenqvist et al., 2003). The size of the area and the quality of the remote sensing data has major influence on the accuracy of the output. For global AGB and carbon stock estimation moderate to coarse resolution remote sensing data (e.g. MODIS) is typically used and at a national or regional scale medium resolution multispectral imagery or SAR data (Baccini et al., 2012; Englhart et al., 2011; Ryan et al., 2012; Saatchi et al., 2011).

Tropical forest ecosystems are one of the largest sinks of carbon, of which tropical peat forests are the highest. It is estimated that the area of tropical peatland is in the range of 30–45 million ha (approximately 10–12 % of the global peatlands) of which 16.8–27.0 million ha are located in Indonesia (Page et al., 2010). With 88.6Gt tropical peatlands are one of the largest near-surface pools of terrestrial organic carbon (IPCC, 2007; Page and Rieley, 1998; Page et al., 2010; Sorensen, 1993). In Indonesia peat accumulates over thousands of years and typically develops convex formed peat domes up to 20 m thick covered by peat swamp forest (Anderson, 1983; Page et al., 2004; Rieley et al., 1996; Rieley and Page, 2005). Due to high deforestation rates and emissions from peat by recurrent fires and bacterial peat decomposition, which is especially observed in the costal lowland areas of Sumatra and Kalimantan, Indonesia is among the largest CO_2 emitters worldwide (Ballhorn et al., 2009; Hooijer at al., 2010; Page et al., 2002).

The main goal of this study was to estimate AGB and to investigate its spatial variability due to natural growth conditions and human impacts along transects of several hundred km in lowland forest ecosystems in the Indonesian province of Central Kalimantan using small-footprint LiDAR remote sensing data. Central Kalimantan comprises a landscape of extensive lowlands with waterlogged peat swamp and lowland dipterocarp forests growing on dry mineral soils. Large-scale logging and peatland drainage resulted in recurrent severe wildfire episodes that destroyed large tracts of these ecosystems and led to huge CO_2 emissions in the past (Ballhorn et al., 2009; Rieley and Page, 2005). Airborne LiDAR is a powerful technique for biomass

BGD
9, 11815–11842, 2012

quantification and monitoring because it provides 3-D information on the forest structure and has been successfully used to derive forest AGB at different scales from single trees (Popescu, 2007; Zhao et al., 2009) to large contiguous forest stands (Asner et al., 2009a; Asner et al., 2010; Lefsky et al., 2002, 2005; Means et al., 1999). Asner et al. (2010) were successful in correlating small-footprint airborne LiDAR to AGB in a tropical lowland forest in Peru. The approach presented in our study on deriving AGB values from airborne LiDAR data follows guidelines proposed by Asner et al. (2010). However there have been no studies so far which investigated the AGB and its variability across large transects in tropical dipterocarp forests.

Especially for the tropical peat swamp forests of Indonesia there is an urgent need to fill knowledge gaps considering AGB values due to different reasons: (i) it is necessary to verify whether the approach on deriving AGB estimates from airborne LiDAR data is applicable to specific forest ecosystems in Indonesia; (ii) as Indonesia is one of the world's biggest emitters of carbon (Ballhorn et al., 2009; Hooijer et al., 2010; Page et al., 2002) it has high potential to negatively influence the global climate if its peatlands are further drained and burned at current rates; (iii) few field measurements considering AGB are available to date as most peatlands in Indonesia are highly inaccessible; (iv) the growing demand for palm oil, due to the biofuel boom, is a serious threat to these ecosystems, since peatlands are one of the only undeveloped and uninhabited near coastal areas in Indonesia; (v) the number of REDD initiatives on peat forests in Indonesia is high (more than 40) and the only certified REDD project under the Voluntary Carbon Standard (VCS) to date in Indonesia is located on a peat swamp forest; (vi) REDD projects require a basic methodology on how to most accurately estimate AGB; and (vii) global climate models will need more reliable data on AGB.

BGD
9, 11815–11842, 2012

2 Materials and methods

2.1 Acquisition and processing of airborne LiDAR data

From 5th to 10th August 2007 airborne LiDAR data was acquired in a flight campaign by Kalteng Consultants and Milan Geoservice GmbH (Fig. 1). Small-footprint full-waveform LiDAR data with a size of 33 178 ha (length of approximately 600 km) was recorded with a Riegl LMS-Q560 Airborne Laser Scanner from a flight altitude of approximately 500 m above ground and a scan angle of 30° (swath width approx. 500 m). The instrument had a pulse rate of up to 100 000 pulses per second, a footprint of 0.25 m, and a wavelength of 1.5 µm (near Infrared). This survey configuration resulted in a nominal point density of 1.4 pt m^{-2}. Under laboratory conditions this system allows height measurements of up to ±0.02 m. The acquired data set has an absolute vertical accuracy of ±0.15 m and horizontal accuracy of ±0.50 m Root Mean Square Error (RMSE). Next step was the filtering of the LiDAR point clouds. This is a crucial step, since the DTM is directly derived from the filtered point clouds. In this study, the filtering was the separation between ground and off-ground LiDAR points, since within the study area all off-ground points consist of vegetation. The applied filtering approach was the hierarchic robust filtering, and the method used to generate the DTMs (1 m resolution) the linear adaptable prediction interpolation (kriging). Both solutions are implemented within the Inpho software package.

Forest inventory data was collected at three sites representative of lowland forest ecosystems from May to August 2008 (Fig. 1). The first site was located in the Sebangau peat swamp forest catchment, with 16 field inventory plots covering tall and low pole peat swamp forests. The second site was situated within Block C of the former Mega Rice Project (MRP), with 20 field inventory plots covering diverse degradation stages of peat swamp forest. The third study site was located in Tumbang Danau and Tewaibaru, with 16 field plots covering logged and unlogged lowland dipterocarp forests. The location of the nested plots was chosen depending on forest type and set in beforehand to guarantee that they lie within the LiDAR point clouds. Four nested

BGD
9, 11815–11842, 2012

plots of one cluster build the corners of a $50 \times 50\,m^2$ square. Trees with a Diameter at Brest Height (DBH) smaller than 7 cm were excluded. The nested plot method is based on three circular plots with different sizes (Pearson et al., 2005). In each of the three circular plots, trees with a certain DBH range were recorded: 7 to 20 cm (4 m radius), 20 to 50 cm (14 m radius), and greater than 50 cm (20 m radius). The sum of the measured parameters of the two smaller nests was multiplied by an expansion factor in order to get the values for the 20 m radius inventory plot (0.13 ha). Local species name and DBH were recorded. Local tree names were translated to the corresponding Latin names through using local expert knowledge, tropical tree databases provided by the World Agroforestry Centre (http://www.worldagroforestrycentre.org/Sea/Products/AFDbases/WD/Index.htm) and Chudnoff (1984), and data from a local herbarium at the Centre for International Co-operation in Management of Tropical Peatland (CIMTROP) in Palangka Raya. Also the species specific wood densities were derived from the above described databases and from IPCC (IPCC, 2006). Some local names, especially of various dipterocarp species, could not be translated, do that an average specific wood density of $0.57\,t\,m^{-3}$ was applied (FAO, 1997). Finally, the AGB values were calculated using an allometric equation for moist tropical forests from Chave et al. (2005) excluding tree height.

2.2 Generation of the regression models

The first step for the generation of the regression models was the creation of a height histogram for every field plot. In order to achieve this, all points within each plot area were normalized to the ground using the DTM as reference. After that, given a predefined height interval (or bin size), the number of points within the given intervals was stored in the form of a histogram. In order to correlate the AGB field observations with the LiDAR metrics, two parameters derived from the height histograms were used. The first, developed for this work, is based on Centroid Height (CH) of the histogram. The second one correlates the AGB with the Quadratic Mean Canopy profile Height

BGD
9, 11815–11842, 2012

(QMCH) (Asner et al., 2010). The first bin of each plot was considered ground return and therefore eliminated from the further processing.

One important parameter in LiDAR surveying is the point density. The acquisition of high point densities is expensive, because it requires the most recent equipment and a slow and low flying aircraft. The real point density can strongly vary across the surveyed area mainly due to stripe overlapping, flight velocity, height variation, target reflectance, and return quality degradation caused by smoke or water vapour in the atmosphere. In order to account for these factors within the regression models, the point density was used for each plot as a weighting factor. Since the point density directly affects the quality of the height histogram, this also directly affects the metrics derived from it (i.e. the CH and QMCH). Usually, the regression models applied for AGB estimations use the AGB as a dependent variable and the LiDAR metrics as independent. In this study, this order was changed because the least-squares solution chosen permitted only weighting the dependent variables, which are treated as observations with known weights – the point densities. For both studied metrics (CH and QMCH) the regression models were derived using the classic approach and the weighted adjustment. After the regression processing, the obtained parameters were transformed in order to obtain an equation that directly determines the AGB based on the LiDAR metrics. In order to verify the influence of point density on the AGB estimation accuracy, a rigorous covariance propagation analysis was performed (see Sect. 2.3).

The biomass estimation models were applied to 600 km (33 178 ha) of LiDAR tracks covering pristine and degraded forest types in Central Kalimantan. The chosen regression model was the CH due to its higher correlation coefficient and lower RMSE. In order to avoid artefacts caused by filtering problems, 20 m of the LiDAR track borders were excluded from the processing.

BGD
9, 11815–11842, 2012

2.3 Rigorous covariance propagation analysis

The basic regression model used in this work correlates the AGB with the LiDAR Metrics (LM) through a power function:

$$\mathrm{AGB} = a \cdot \mathrm{LM}^{b} \tag{1}$$

Although, in order to permit LiDAR metrics weighting, it is necessary to rewrite Eq. (1) with LM as dependent variable:

$$\mathrm{LM} = k \cdot \mathrm{AGB}^{w} \tag{2}$$

In this form, the LiDAR metrics can be treated as observations and weighted with the correspondent LiDAR point density within a non-linear least-squares solution. After the regression processing, the residuals of the observations can be determined as well as the covariance matrix of the parameters k and w ($\mathbf{\Sigma}_{kw}$). Now it is necessary to transform the parameters k and w (Eq. 2) into a and b (Eq. 1), which actually correlate the LiDAR metrics with the AGB:

$$a = \left(1/k\right)^{1/w} \tag{3}$$

$$b = 1/w \tag{4}$$

In order to perform a rigorous AGB accuracy estimation, it is necessary to determine the covariance matrix of the parameters a and b ($\mathbf{\Sigma}_{ab}$) though a covariance propagation:

$$\mathbf{\Sigma}_{ab} = G \cdot \mathbf{\Sigma}_{kw} \cdot G^{T} \tag{5}$$

Where:

$$G = \begin{bmatrix} \partial a/\partial k & \partial a/\partial w \\ \partial b/\partial k & \partial b/\partial w \end{bmatrix} = \begin{bmatrix} -1/k^{\frac{w+1}{w}} \cdot w & \ln(k)/k^{\frac{1}{w}} \cdot w^{2} \\ 0 & -1/w^{2} \end{bmatrix} \tag{6}$$

BGD
9, 11815–11842, 2012

Returning to Eq. (1), one can write a new covariance propagation equation:

$$\mathbf{\Sigma}_{\mathrm{AGB}} = \sigma^2_{\mathrm{AGB}} = D \cdot \mathbf{\Sigma}_{\mathrm{LM},ab} \cdot D^T \tag{7}$$

Considering all terms on the right side of the Eq. (1) as parameters, one comes to:

$$D = \left[a \cdot b \cdot \mathrm{LM}^{b-1} \ \mathrm{LM}^b \ a \cdot \mathrm{LM}^b \cdot \ln(\mathrm{LM}) \right] \tag{8}$$

Take $\mathbf{\Sigma}_{\mathrm{LM},ab}$ as the extended covariance matrix:

$$\mathbf{\Sigma}_{\mathrm{LM},ab} = \begin{bmatrix} \sigma^2_{\mathrm{LM}} & 0 & 0 \\ 0 & \sigma^2_a & \sigma_{ab} \\ 0 & \sigma_{ab} & \sigma^2_b \end{bmatrix} \tag{9}$$

Solving Eq. (7) with Eqs. (8) and (9) and denoting the point density ρ, one comes to the final AGB standard deviation (σ_{AGB}) estimation model:

$$\sigma_{\mathrm{AGB}} = \sqrt{A/\sqrt{\rho} + B + C} \tag{10}$$

With:

$$A = \left(a \cdot b \cdot \mathrm{LM}^{b-1} \right)^2 \tag{11}$$

$$B = \mathrm{LM}^b \cdot \left(\mathrm{LM}^b \cdot \sigma^2_a + \sigma_{ab} \cdot \left(a \cdot \mathrm{LM}^b \cdot \ln(\mathrm{LM}) \right) \right) \tag{12}$$

$$C = \left(a \cdot \mathrm{LM}^b \cdot \ln(\mathrm{LM}) \right) \cdot \left(\sigma_{ab} \cdot \mathrm{LM}^b + \sigma^2_b \left(a \cdot \mathrm{LM}^b \cdot \ln(\mathrm{LM}) \right) \right) \tag{13}$$

Equations (10) to (13) were applied to the CH and QMCH models derived in this work.

BGD
9, 11815–11842, 2012

2.4 Comparison between optical remote sensing and LiDAR for AGB estimation

Prior to the image classification, the Landsat imagery (ETM+ 118-62, 5 August 2007) was atmospherically corrected using ATCOR (Richter, 1997). The land cover classification for the 1 million ha study area was implemented using an object-based image analysis approach (software eCognition, Trimble GeoSpatial, Munich, Germany). In a first step, this approach generates image objects from spatially adjacent pixels with similar spectral values, which are then classified by a user defined rule-set. In order to differentiate primary and secondary forests, a pixel-based spectral mixture analysis (SMA) was applied to the data. SMA have a high potential to derive forest degradation from remote sensing data (Asner et al., 2009b; Matricardi et al., 2010; Souza at al., 2005). A linear SMA assumes that each pixel spectrum is a linear combination of a finite number of endmembers (Adams et al., 1986). The results of a SMA, i.e. scaled sub-pixel fractions representing photosynthetically active vegetation, non-photosynthetic vegetation (NPV), soil and shade, were used to derive disturbed forest areas. The final land cover classification had an overall accuracy of 89 % with a Kappa coefficient of 0.88.

Next the LiDAR AGB estimates for 28 284 ha of the LiDAR tracks, covering only peatland, were quantitatively compared with the Landsat classification. The AGB values of the land cover types were derived from site specific field inventory data ($n = 53$), regional literature estimates (literature values for the Indo-Malayan archipelago), and IPCC default values (IPCC, 2006) and assigned to the land cover types classified in the satellite imagery, which is a method often used (Gibbs et al., 2007). Site specific field inventory data represent Tier 2/3, regional literature estimates Tier 2, and IPCC default values Tier 1 of the IPCC Guidelines for National Greenhouse Gas Inventories (IPCC, 2006). Higher Tiers represent higher levels of precision and accuracy in AGB estimation (IPCC, 2006). Finally the average LiDAR AGB estimates within the LiDAR tracks for the land cover classes on peatlands were extrapolated to the 1 million ha study area and compared to the AGB results based on the site specific field inventory data, regional literature estimates, and IPCC default values.

BGD
9, 11815–11842, 2012

For the class burned it has to be noted that the Landsat classification also includes burned areas where regrowth already took place for more than 3 yr. On the other hand the field plots (but also the regional literature estimates and the IPCC default values) where collected in fires scars not older than 3 yr. This explains the difference in AGB between the LiDAR estimates and the estimates based on the site specific field inventory data, regional literature estimates, and IPCC default values (Tables 1 and 2). As both, area and AGB, of this class are small this does not have big impact on the overall results (Tables 1 and 2).

3 Results

The LiDAR point clouds were analysed using both techniques presented in Sect. 2.3 (CH and QMCH). These parameters were correlated to field estimated AGB values (0.13 ha) in order to establish robust biomass estimation models. The biomass estimation models were applied to 600 km (33 178 ha) of LiDAR tracks covering pristine and degraded forest types in Central Kalimantan

Four main forest types – tall peat swamp forest, low pole peat swamp forest, degraded forest (logged or burned) and lowland *dipterocarp* forest – were investigated. Figure 2 shows four typical field plots, their LiDAR height profiles with vegetation heights, and the derived LiDAR height histograms, which illustrate the structural differences between the different forest types and the impact of degradation.

Figure 3a shows the results for the regression using the CH as input. A high correlation coefficient ($R^2 = 0.88$; RMSE = ±13.79 t 0.13 ha^{-1}; PPR = ±14.98 t 0.13 ha^{-1}) was obtained when the LiDAR point densities per square meter (pt m^{-2}) were treated as weight during the regression. The derived coefficient of determination is comparable with those reported in other studies of tropical forests (Asner et al., 2009a, 2010; Drake et al., 2002). Also for the QMCH a high correlation was obtained ($R^2 = 0.84$) when applying the LiDAR point density as weight (Fig. 3b). In both cases, the use of the LiDAR point densities as weight improved the regression models.

BGD
9, 11815–11842, 2012

The costs of LiDAR surveying depend on the point density. To assess the influence of the LiDAR point density on the quality of the AGB estimation, a rigorous covariance propagation analysis was performed (see Sect. 2.2). The results (Fig. 3c) suggest that LiDAR surveying with more than 4 pt m^{-2} does not significantly improve the AGB regression models. On the other hand surveying with less than 1 pt m^{-2} may lead to significant inaccuracies, so that we conclude that surveying with a point density between 2 and 4 pt m^{-2} may show the best cost-benefit ratio.

To validate the proposed AGB estimation, we determined the Predictive Power of the Regression (PPR) as proposed by Asner et al. (2010). 5000 iterations were performed randomly leaving 10 % of the plots out of the regression as control. The Root Mean Square Error (RMSE) after this iterative process was about 1 t/0.13 ha higher than the RMSE determined using all plots in the regression. These results are similar to the ones presented by Asner et al. (2010).

Next the spatial variability of AGB along the 600 km LiDAR tracks was analyzed. Through applying the CH based regression model it was possible to illustrate AGB variability linked to local soil properties and water logged conditions and the impact of previous logging operation and fire with high spatial resolution. Figure 4 shows a 10 km long (408 ha) LiDAR transect covering pristine and logged peat swamp forest (location of this transect is shown in Fig. 4). Figure 4a shows a Landsat scene acquired in the year 2000 where forests appear in green and logging impact in pink colors. Historical Landsat imagery suggests that logging occurred here in the year 1997. After 1998 all logging operation has been terminated. In the 2007 Landsat image this previous logging activity is no longer visible (Fig. 4b) but still detectable in the LiDAR AGB profile shown in Fig. 4d (black, black arrows). There is an AGB variation of up to 150 % in logged and pristine peat swamp forest (20–50 t 0.13 ha^{-1}) (Fig. 4d). The AGB is approximately 35 % lower than in adjacent areas with little or no logging impact although there has been 10 yr of forest regrowth. LiDAR AGB spatial profils clearly show the ability of airborne LiDAR to assess AGB variability with high spatial resolution and also

BGD
9, 11815–11842, 2012

detect former logging activity which is no longer visible in recent multispectral satellite imagery (Fig. 4a, b, and d).

A standard method to estimate AGB is to assign AGB values to a land cover classification based on multispectral satellite imagery (indirect method) (Gibbs et al., 2007). In the case of the LiDAR track shown in Fig. 4, the Landsat based classification only allows for the discrimination between two land cover classes, i.e. peat swamp forest pristine and logged. In Fig. 4c the LiDAR AGB estimates are superimposed on the Landsat based land cover classification. Figure 4d shows a comparison between AGB estimates from LiDAR (black), site specific field inventory data (orange), regional literature estimates (yellow), and IPCC default values (red). From Fig. 4c, d it is clear that the spectral reflectance in Landsat imagery does not represent the spatial AGB heterogeneity. Thereby, AGB losses by logging will be undetected or underestimated. In this study it leads to a serious overestimation of the AGB by the indirect method. Figure 5 shows more examples of the observed AGB variability. In Fig. 5a the location of these profiles within the study area is shown and superimposed on Landsat image acquired in the year 2007. Green colors indicate lowland *dipterocarp* forest, while pink and red colors indicate sparse vegetation. Fire scars from fires several years back in time appear in light green and recent fire scars from the year 2006 appear in red. AGB profile 2 in Fig. 5b transects two areas of previous logging activity. The LiDAR data set indicates lower AGB values in logged areas which are not detectable in the Landsat image and the land cover based estimate. AGB profile 3 (Fig. 5c) transects a fire scar which was created during the severe fire disaster in 1997. Here the Landsat based estimate is higher than the LiDAR estimate. Forest regrowth was much slower than expected and thus the AGB is overestimated. AGB profile 4 (Fig. 5d) covers peat swamp forest and two fire scars from different years (2002 in the west and 2006 in the east) located on a higher section of the elevated peat dome. The LiDAR AGB indicates significantly lower AGB values for the peat swamp forest as in other areas in the study site or as indicated by standard AGB values most likely caused by unfavorable growth conditions.

BGD
9, 11815–11842, 2012

Table 1 presents the results of the comparison between the LiDAR AGB estimates for the LiDAR tracks and Table 2 the up-scaling of these estimates to the whole study area compared to other methods and standard AGB values. The variation of the LIDAR AGB estimates for different land cover classes (based on the Landsat classification) is noticeable here as well (Tables 1 and 2). For areas classified as peat swamp forest pristine, representing 36 % of all LiDAR track area and constituting approximately 65 % of the total estimated AGB, this variation can be up to 140 % (Table 1). Furthermore, the LiDAR AGB estimates for this class are 38 %, 96 %, and 120 % lower than using values assigned to this class based on the site specific field inventory data, regional literature estimates, and IPCC default values, respectively (Table 1). Similar relationships were found in other land cover classes and therefore the direct LiDAR based AGB estimate is in total 43 % (site specific field inventory data), 102 % (regional literature estimates), 137 % (IPCC default values) lower than the indirect method considering the 1 million ha study area (Table 2). This overestimation is higher than that shown by Asner et al. (2010) who observed a 33 % lower regional LiDAR based carbon estimate than by a default approach based on average IPCC (IPCC, 2006) carbon values assigned to biomes in the Peruvian Amazon.

4 Discussion

Our results confirm that the use of airborne LiDAR data is the most reliable solution for AGB and carbon stock estimates (Asner et al., 2009a, 2010; Lefsky et al., 2002, 2005; Means et al., 1999; Popescu, 2007; Zhao et al., 2009;). Despite its relatively high operation costs for large scale mapping this approach produces the most accurate estimates of forest carbon stocks in that it captures the natural spatial variability and previous impacts like logging. Global estimates based on low and medium resolution satellite data (Baccini et al., 2012; Saatchi et al., 2011) do not capture the local variability in forest AGB (natural and human-caused) which is required for REDD+ project Measuring, Reporting, and Verification (MRV) systems. A “benchmark” map of

BGD
9, 11815–11842, 2012

biomass carbon stock for the tropics, based on a combination of in situ inventory plots, satellite LiDAR data, and optical and microwave imagery (1 km resolution), showed that especially for the peat forest areas of Central Kalimantan the uncertainty in biomass carbon stock estimates was very high (> ±45 %) (Saatchi et al., 2011). This high uncertainty, the limited amount of in situ field measurements in South East Asean tropical forests (especially in tropical peat swamp forests), and the inability of high and medium multispectral resolution satellite instruments such as Landsat to quantify historic forest disturbance show the importance to derive more accurate AGB estimates in these inaccessible ecosystems. In combination with high resolution satellite imagery airborne LiDAR could be a cost effective approach to derive more accurate regional maps on forest carbon densities (Asner et al., 2010). Furthermore the new approach presented here through using the CH and incorporating LiDAR point densities as weight has the capability to improve current estimates on AGB spatial variability across different forest types and degradation levels also in other tropical biomes and to assist the efforts in up-scaling LiDAR derived AGB estimates to large-scale geographic areas.

There exists a considerable natural variability of AGB up to 140 % within the same forest type due to varying environmental conditions. For example we found that in water logged conditions the AGB is significantly lower than in drier locations. AGB reduction by logging dating back more than 10 yr can still be assessed by LiDAR but not by multispectral satellite imagery available for that period in time.

The up-scaling of LiDAR AGB estimates to a large area of 1 million ha (59 % peat swamp forest) showed an overestimation of 46 %, 102 %, and 137 % compared to the indirect method based on a Landsat land cover map and site specific field inventory data, regional literature values, and IPCC default values (Table 2). If the whole area would be completely deforested (a likely scenario for the near future) this would lead to an overestimation 63, 148, 198 Mega tons of CO_2 (34, 81, 108 Mega tons of AGB; conversion factor from AGB to carbon 0.5 (IPCC, 2006).

BGD
9, 11815–11842, 2012

Especially for the carbon rich tropical peat swamp forests this finding is of high importance because this ecosystem is disappearing with alarming rates due to the conversion to oil palm plantations established to meet the demands for biofuels. By converting peat swamp forests into bio fuel plantations more carbon will be released than it is saved by using biofuels (Dewi et al., 2009).

For REDD+ activities default values or indirect approaches to determine AGB is not sufficiently reliable and leads to inaccurate carbon stock estimates and consequently to excessive carbon credits and compensation payments

Acknowledgements. We would like to thank Suwido Limin and his team from CIMTROP for the logistic support during the field inventory and Sampang Gaman (CIMTROP) and Simon Husson (Orang Utan Tropical Peatland Project, OUTROP) for providing tree species lists. Further we would like to thank FORRSA (Forest Restoration and Rehabilitation in Southeast Asia) project of the EU-funded Asia Link programme for financially supporting the field trips to Indonesia. The LiDAR data set was acquired by Kalteng Consultants.

References

Adams, J. B., Smith, M. O., and Johnson, P. E.: Spectral mixture modeling: a new analysis of rock and soil types at the Viking Lander 1 site, J. Geophys. Res., 91, 8090–8112, 1986.

Anderson, J. A. R.: Ecosystems of the World 4b-Mires: Swamp, Bog, Fern and Moor, edited by: Gore, A. J. P., Elsevier, Amsterdam, The Netherlands, 181–199, 1983.

Asner, G. P., Hughes, R. F., Varga, T. A., Knapp, D. E., and Kennedy-Bowdoin, T.: Environmental and biotic controls over aboveground biomass throughout a tropical rain forest, Ecosystems, 12, 261–278, 2009a.

Asner, G. P., Knapp, D. E., Balaji, A., and Paez-Acosta, G.: Automated mapping of tropical deforestation and forest degradation: CLASlite, J. Appl. Remote Sens., 3, 033543, doi:10.1117/1.3223675, 2009b.

Asner, G. P., Powell, G. V. N., Mascaro, J., Knapp, D. E., Clark, J. K., Jacobson, J., Kennedy-Bowdoin, T., Balaji, A., Paez-Acosta, G., Victoria, E., Secada, L., Valqui, M., and Hughes, R. F.: Highresolution forest carbon stocks and emissions in the Amazon, P. Natl. Acad. Sci. USA, 107, 16738–16742, 2010.

BGD
9, 11815–11842, 2012

Baccini, A., Goetz, S. J., Walker, W. S., Laporte, N. T., Sun, M., Sulla-Menashe, D., Hackler, J., Beck, P. S. A., Dubayah, R., Friedl, M. A., Samanta, S., and Houghton, R. A.: Estimated carbon dioxide emissions from tropical deforestation improved by carbon-density maps, Nature Clim. Change, 2, 182–185, doi:10.1038/nclimate1354, 2012.

Ballhorn, U., Siegert, F., Mason, M., and Limin, S.: Derivation of burn scar depths and estimation of carbon emissions with LIDAR in Indonesian peatlands, P. Natl. Acad. Sci. USA, 106, 21213–21218, 2009.

Chave, J., Andalo, C., Brown, S., Cairns, M. A., Chambers, J. Q., Eamus, D., Folster, H., Fromard, F., Higuchi, N., Kira, T., Lescure, J.-P., Nelson, B. W., Ogawa, H., Puig, H., Riera, B., and Yamakura, T.: Tree allometry and improved estimation of carbon stocks and balance in tropical forests, Oecologia, 145, 87–99, 2005.

Chudnoff, M.: Tropical Timbers of the World, Agriculture Handbook 607, US Department of Agriculture, Forest Service, Forest Products Laboratory, Madison, WI, USA, 1984.

Dewi, S., Khasanah, N., Rahayu, S., Ekadinata, A., and Van Noordwijk, M.: Carbon Footprint of Indonesian Palm Oil Production: A Pilot Study, World Agroforestry Centre (ICRAF), Bogor, Indonesia, 2009.

Drake, J. B., Dubayah, R. O., Clark, D. B., Knox, R. G., Blair, J. B., Hofton, M. A., Chazdon, R. L., Weishampel, J. F., and Prince, S. D.: Estimation of tropical forest structural characteristics using large-footprint lidar, Remote Sens. Environ., 79, 305–319, 2002.

Drake, J. B., Knox, R. G., Dubayah, R. O., Clark, D. B., Condit, R., Blair, J. B., and Hofton, M.: Above-ground biomass estimation in closed canopy Neotropical forests using lidar remote sensing: factors affecting the generality of relationships, Glob. Ecol. Biogeogr., 12, 147–159, 2003.

Englhart, S., Keuck, V., and Siegert, F.: Aboveground biomass retrieval in tropical forests – the potential of combined X- and L-band SAR data use, Remote Sens. Environ., 115, 1260–1271, 2011.

FAO: Estimating Biomass and Biomass Change of Tropical Forests: A Primer, Food and Agriculture Organization of the United Nations, Rome, Italy, FAO Forestry Paper 134, 1997.

FAO: Global Forest Resources Assessment 2005, Food and Agriculture Organization of the United Nations, Rome, Italy, FAO Forestry Paper 147, 2006.

Gibbs, H. K., Brown, S., Niles, J. O., Foley, J. A.: Monitoring and estimating tropical forest carbon stocks: making REDD a reality, Environ. Res. Lett,. 2, 045023, doi:10.1088/1748-9326/2/4/045023, 2007.

BGD
9, 11815–11842, 2012

Hansen, M. C., Stehman, S. V., Potapov, P. V., Arunarwati, B., Stolle, F., and Pittman, K.: Quantifying changes in the rates of forest clearing in Indonesia from 1990 to 2005 using remotely sensed data sets, Environ. Res. Lett., 4, 034001, doi:10.1088/1748-9326/4/3/034001, 2009.

Hooijer, A., Page, S., Canadell, J. G., Silvius, M., Kwadijk, J., Wösten, H., and Jauhiainen, J.: Current and future CO_2 emissions from drained peatlands in Southeast Asia, Biogeosciences, 7, 1505–1514, doi:10.5194/bg-7-1505-2010, 2010.

IPCC: Guidelines for National Greenhouse Gas Inventories, edited by: Eggleston, H. S., Buendia, L., Miwa, K., Ngara, T., and Tanabe, K., National Greenhouse Gas Inventories Programme, Kamiyamaguchi, Japan, 2006.

IPCC: Climate Change 2007: The Physical Science Basis. Contribution of Working Group I to the Fourth Assessment Report of the Intergovernmental Panel on Climate Change, edited by: Solomon, S., Qin, D., Manning, M., Chen, Z., Marquis, M., Averyt, K. B., M. Tignor, M., and Miller, H. L., Cambridge University Press, Cambridge, UK, 2007.

Langner, A. and Siegert, F.: Spatiotemporal fire occurence in Borneo over a period of 10 years, Glob. Change Biol., 15, 48–62, 2009.

Langner, A., Miettinen, J., and Siegert, F.: Land cover change 2002–2005 in Borneo and the role of fire derived from MODIS imagery, Glob. Change Biol., 13, 1–12, 2007.

Lefsky, M. A., Cohen, W. B., Harding, D. J., Parker, G. G., Acker, S. A., and Gower, S. T.: Lidar remote sensing of above-ground biomass in three biomes, Global Ecol. Biogeogr., 11, 393–399, 2002.

Lefsky, M. A., Harding, D. J., Keller, M., Cohen, W. B., Carabajal, C. C., Espirito-Santo, F. D. B., Hunter, M. O., and De Oliveira Jr., R.: Estimates of forest canopy height and aboveground biomass using ICESat, Geophys. Res. Lett., 32, L22S02, doi:10.1029/2005GL023971, 2005.

Matricardi, E. A. T., Skole, D. L., Pedlowski, M. A., Chomentowski, W., and Fernandes, L. C.: Assessment of tropical forest degradation by selective logging and fire using Landsat imagery, Remote Sens. Environ., 114, 1117–1129, 2010.

Means, J. E., Acker, S. A., Harding, D. J., Blair, J. B., Lefsky, M. A., Cohen, W. B., Harmon, M. E., and McKee, W. A.: Use of large-footprint scanning airborne lidar to estimate forest stand characteristics in the Western Cascades of Oregon, Remote Sens. Environ., 67, 298–308, 1999.

Page, S. E. and Rieley, J. O.: Tropical peatlands: a review of their natural resource functions with particular reference to Southeast Asia, Int. Peat J., 8, 95–106, 1998.

BGD
9, 11815–11842, 2012

Page, S. E., Siegert, F., Rieley, J. O., Boehm, H.-D., V., Jaya, A., and Limin, S.: The amount of carbon released from peat and forest fires in Indonesia during 1997, Nature, 420, 61–65, 2002.

Page, S. E., Wüst, R. A. J., Weiss, D., Rieley, J. O., Shotyk, W., and Limin, S. H.: Late Pleistocene and Holocene carbon accumulation and climate change from an equatorial peat bog (Kalimantan, Indonesia): implications for past, present and future carbon dynamics, J. Quaternary Sci., 19, 625–635, 2004.

Page, S. E., Rieley, J. O., and Banks, C. J.: Global and regional importance of the tropical peatland carbon pool, Glob. Chang. Biol., 17, 798–818, 2010.

Pearson, T., Walker, S., and Brown, S.: Sourcebook for Land Use, Land-Use Change and Forestry Projects, Winrock International, Little Rock, AR, USA, 2005.

Popescu, S. C.: Estimating biomass of individual pine trees using airborne lidar, Biomass and Bioenergy, 31, 646–655, 2007.

Rieley, J. O. and Page, S. E. (eds.): Wise Use of Tropical Peatlands: Focus on Southeast Asia, ALTERRA, Wageningen, The Netherlands, 2005.

Rieley, J. O., Ahmad-Shah, A. A., and Brady, M. A.: The extent and nature of tropical peat swamps, in: Tropical Lowland Peatlands of Southeast Asia: Proceedings of a Workshop on Integrated Planning and Management of Tropical Lowland Peatlands held at Cisarua, Indonesia, 3–8 July 1992, edited by: Maltby, E., Immirzi, C. P., and Safford, R. J., IUCN, Gland, Switzerland, 17–53, 1996.

Richter, R.: Correction of atmospheric and topographic effects for high spatial resolution imagery, Int. J. Remote Sens., 8, 1099–1111, 1997.

Rosenqvist, A., Milne, A., Lucas, R., Imhoff, M., and Dobson, C.: A review of remote sensing technology in support of the Kyoto Protocol, Environ. Sci. Policy, 6, 441–455, 2003.

Ryan, C. M., Hill, T., Woollen, E., Ghee, C., Mitchard, E., Cassells, G., Grace, J., Woodhouse, I. H., and Williams, M.: Quantifying small-scale deforestation and forest degradation in African woodlands using radar imagery, Glob. Change Biol., 18, 243–257, 2012.

Saatchi, S. S., Harris, N. L., Brown, S., Lefsky, M., Mitchard, E. T. A., Salas, W., Zutta, B. R., Buermann, W., Lewis, S. L., Hagen, S., Petrova, S., White, L., Silman, M., and Morel, A.: Benchmark map of forest carbon stocks in tropical regions across three continents, P. Natl. Acad. Sci. USA, 108, 9899–9904, 2011.

Siegert, F., Rücker, G., Hinrichs, A., and Hoffmann, A.: Increased fire impacts in logged over forests during El Niño driven fires, Nature, 414, 437–440, 2001.

BGD
9, 11815–11842, 2012

Sorensen, K. W.: Indonesian peat swamp forests and their role as a carbon sink, Chemosphere, 27, 1065–1082, 1993.

Souza, C. M., Roberts Jr., D. A., and Cochrane, M. A.: Combining spectral and spatial information to map canopy damage from selective logging and forest fires, Remote Sens. Environ., 98, 329–343, 2005.

Van der Werf, G. R., Morton, D. C., DeFries, R. S., Olivier, J. G. J., Kasibhatla, P. S., Jackson, R. B., Collatz, G. J., and Randerson, J. T.: CO_2 emissions from forest loss, Nat. Geosci., 2, 737–738, 2009.

Zhao, K. G., Popescu, S., and Nelson, R.: Lidar remote sensing of forest biomass: a scale-invariant estimation approach using airborne lasers, Remote Sens. Environ., 113, 182–196, 2009.

BGD
9, 11815–11842, 2012

Table 1. Above Ground Biomass (AGB) comparison between the LiDAR based estimations and AGB estimations where AGB values were based on site specific field inventory data (Field plots), regional literature estimates (Literature), and IPCC default values (IPCC) and the attributed to land cover classes, derived from a Landsat (multispectral satellite) classification, for the peatlands within the LiDAR stripes of the 1 million ha study area (Mt = Megaton).

Class			Averaged AGB (t/0.13 ha)				Total AGB (Mt)							Difference (%)		
Name	Area (ha)	%	LiDAR	Field Plots	Literature	IPCC	LiDAR	%	Field Plots	%	Literature	%	IPCC	%	LiDAR – Field Plots	LiDAR – Literature	LiDAR – IPCC
Peat swamp forest pristine	9724.53	36	20.67 (±14.68)	28.62 (±9.48)	40.56 (±24.57)	45.50	1.546	65	2.141 (±0.709)	62	3.034 (±1.838)	63	3.404	61	38	96	120
Peat swamp forest logged	7094.17	27	13.78 (±12.12)	23.20 (±9.53)	30.42 (±24.57)	36.40	0.752	32	1.266 (±0.520)	37	1.660 (±1.341)	34	1.986	35	68	121	164
Bushland/ Regrowth	2828.97	11	1.86 (±5.16)	1.64 (±1.08)	3.90 (±7.02)	9.10	0.040	2	0.036 (±0.023)	1	0.085 (±0.153)	2	0.198	4	−12	110	390
Grassland/ Fern	5543.88	21	0.33 (±2.09)	0.43 (±1.35)	1.56 (±1.75)	0.81	0.014	1	0.019 (±0.058)	1	0.067 (±0.074)	1	0.034	1	31	370	143
Burned	1509.79	6	1.36 (±3.50)	0.09 (±1.09)	0.00	0.00	0.016	1	0.001 (±0.013)	0	0.00	0	0.00	0	−93	−100	−100
Total	**26 701.34**	**100**					**2.369**	**100**	**3.462 (±2.596)**	**100**	**4.845 (±6.736)**	**100**	**5.622**	**100**	**46**	**105**	**137**

BGD
9, 11815–11842, 2012

Table 2. Above Ground Biomass (AGB) comparison between the LiDAR based estimations and AGB estimations where AGB values were based on site specific field inventory data (Field plots), regional literature estimates (Literature), and IPCC default values (IPCC) and the attributed to land cover classes, derived from a Landsat (multispectral satellite) classification, for the peatlands for the whole 1 million ha study area (Mt = Megaton).

Class			Total AGB (Mt)								Difference (%)		
Name	Area (ha)	%	LiDAR	%	Field Plots	%	Literature	%	IPCC	%	LiDAR – Field Plots	LiDAR – Literature	LiDAR – IPCC
Peat swamp forest pristine	351 588.32	39	55.912 (±39.702)	71	77.408 (±25.639)	68	109.696 (±66.450)	69	123.056	66	38	96	120
Peat swamp forest logged	186 130.60	20	19.725 (±17.353)	25	33.201 (±13.645)	29	43.555 (±35.179)	27	52.117	28	68	121	164
Bushland/ Regrowth	154 197.54	17	2.205 (±6.120)	3	1.943 (±1.281)	2	4.626 (±8.327)	3	10.794	6	−12	110	390
Grassland/ Fern	154 108.55	17	0.394 (±2.478)	0	0.515 (±1.600)	0	1.849 (±2.075)	1	0.955	1	31	370	143
Burned	65 425.08	7	0.682 (±1.761)	1	0.047 (±0.549)	0	0.00 (±0.00)	0	0.00	0	−93	−100	−100
Total	911 450.10	100	78.918 (±127.752)	100	113.115 (±83.841)	100	159.725 (±220.134)	100	186.922	100	43	102	137

BGD
9, 11815–11842, 2012

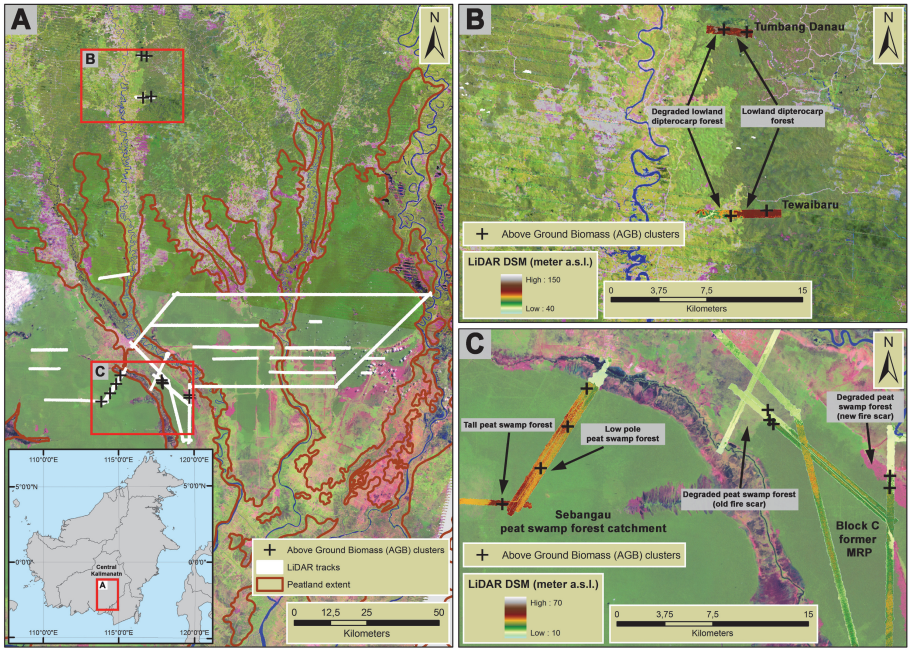

Fig. 1. Location of the LiDAR tracks and Above Ground Biomass (AGB) clusters (see methods) (0.13 ha, indicated by black +) in Central Kalimantan, Indonesia, superimposed on a Landsat image (ETM+ 118-61, 2009-05-22 and ETM+ 118-62, 5 August 2007; bands 5-4-3 and both scenes were gap filled). The red rectangles show the location of A, B, and C. In B and C also the LiDAR derived Digital Surface Models (DSM) are shown.

BGD
9, 11815–11842, 2012

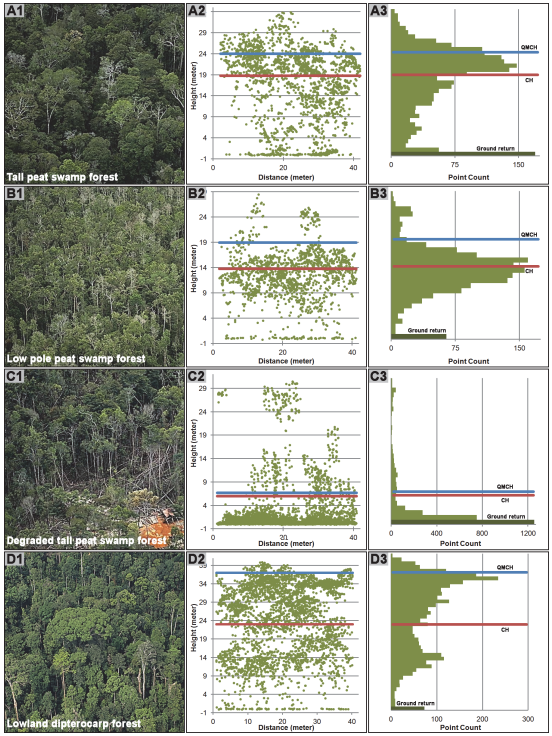

Fig. 2. Sample data set for each of the four investigated forest types. **(A1)** to **(A3)** show tall peat swamp forest (AGB = 57.61 t 0.13 ha^{-1}, LiDAR point density = 1.5 pt m^{-2}, Centroid Height (CH) = 18.7 m, Quadratic Mean Canopy profile Height (QMCH) = 24.0 m). Note that CH and QMCH are in the upper canopy of the forest. **(B1)** to **(B2)** show low pole peat swamp forest (AGB = 19.12 t 0.13 ha^{-1}, LiDAR point density = 1.1 pt m^{-2}, CH = 13.7 m, QMCH = 18.9 m). **(B3)** shows the forest structure (a small peak at about 24 m representing emergent trees and a large peak at about 14 m representing the main canopy layer). **(C1)** to **(C3)** show logged tall peat swamp forest (AGB = 5.05 t 0.13 ha^{-1}, point density = 2.9 pt m^{-2}, CH = 5.8 m, QMCH = 6.2 m). The small peak in **(C2)** at about 26 m height indicates remaining tall trees. **(C3)** clearly shows the predominant ground return. CH and QMCH are located in similar heights. **(D1)** to **(D3)** show lowland *dipterocarp* forest (AGB = 108.20 t 0.13 ha^{-1}, LiDAR point density = 2.3 pt m^{-2}, CH = 25.3 m, QMCH = 35.3 m). The two peaks in **(D3)** (at about 14 m and 34 m) indicate a complex multi-layered forest structure.

BGD
9, 11815–11842, 2012

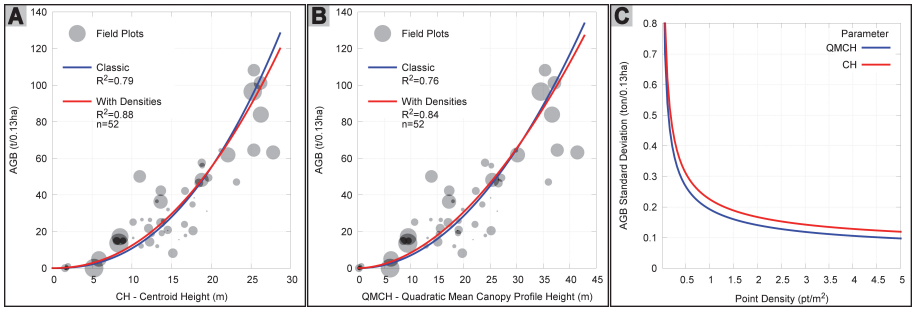

Fig. 3. Biomass regression and rigorous covariance propagation analysis results. **(A)** In red the Centroid Height (CH) based regression model with LiDAR point density weighting ($AGB = 0.0865 \times CH^{2.1564}$; $R^2 = 0.88$; Root Mean Square Error (RMSE) = ±13.79 t 0.13 ha^{-1}; Predictive Power of the Regression (PPR) = ±14.98 t 0.13 ha^{-1}) and in blue without weighting ($AGB = 0.0484 \times CH^{2.3494}$; $R^2 = 0.79$; RMSE = ±16.06 t 0.13 ha^{-1}; PPR = ±17.43 t 0.13 ha^{-1}). **(B)** In red the Quadratic Mean Canopy profile Height (QMCH) based regression model with LiDAR point density weighting ($AGB = 0.1150 \times QMCH^{1.8656}$; $R^2 = 0.84$) and in blue without weighting ($AGB = 0.0660 \times QMCH^{2.0277}$; $R^2 = 0.76$). The circle size in **(A)** and **(B)** represents the point densities (the smallest about 0.2 pt m^{-2} and the biggest about 3.5 pt m^{-2}). **(C)** Standard deviation behaviour estimation curves for CH and QMCH based regression models (derived from the covariance propagation analysis).

BGD
9, 11815–11842, 2012

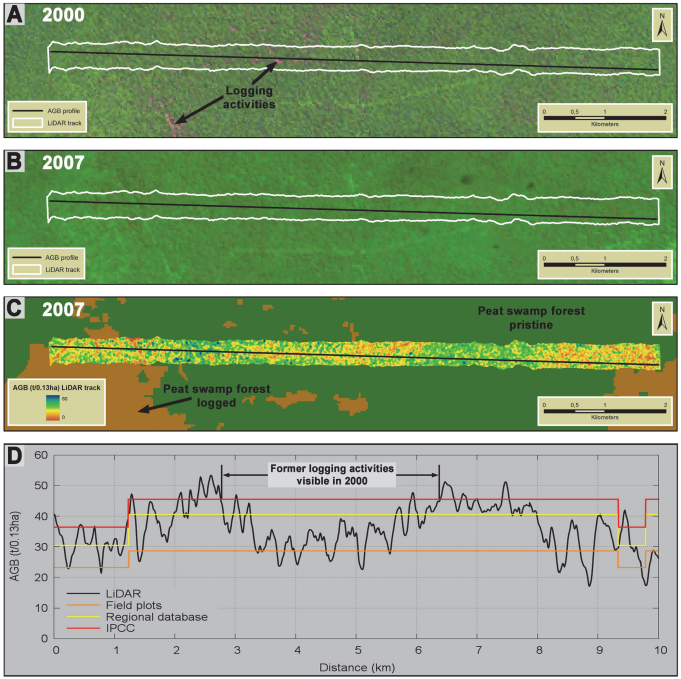

Fig. 4. AGB results shown for a LiDAR track covering 10 km in the Sebangau peat swamp forest catchment. Location of this LiDAR track is shown in Fig. 4 (AGB profile 1). **(A)** Extent of the LiDAR track and the location of the AGB profile of **(D)** superimposed on a Landsat scene from the year 2000 (ETM+ 118-62, 16 July 2000, bands 5-4-3). Green represents forest cover and logging activities are visible as pink dots near to straight line features (logging railways). **(B)** Extent of the LiDAR track and the location of the AGB profile of **(D)** superimposed on a Landsat scene from the year 2007 (ETM+ 118-62, 5 August 2007; bands 5-4-3; gap filled). The logging activities are not visible anymore. **(C)** LiDAR AGB regression results superimposed on the Landsat classification (green = peat swamp forest pristine, brown = peat swamp forest logged). **(D)** AGB variability measured by LiDAR (black) and the corresponding AGB estimates attributed to the land cover types of the Landsat classification. Site specific inventory data (Field plots) = orange, regional literature estimates (Regional database) = yellow, and IPCC default values (IPCC) = red. Black arrows indicate the extent of the logging activities seen in **(A)**.

BGD
9, 11815–11842, 2012

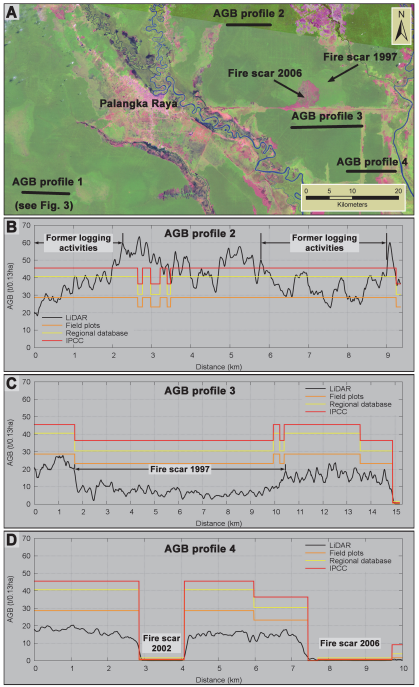

Fig. 5. Examples of different AGB profiles where LiDAR based AGB estimates are compared to the AGB values attributed to the land cover classes from the Landsat classification on peatlands within the LiDAR stripes. Three different sources for AGB values were attributed to the land cover classes: site specific field inventory data (Field plots, orange), regional literature estimates (Regional database, yellow), and IPCC default values (IPCC, red). AGB profile 1 is described in more detail in Fig. 3. **(A)** Location of the AGB profiles within the study area superimposed on Landsat imagery from the year 2007. **(B)** AGB profile 2 (9.5 km long) covers two areas of former logging activities (0.0–2.2 km and 5.9–9.0 km) within a peat swamp forest. Here the AGB variability within the forest and the lower AGB values in the logging areas is visible in the LiDAR estimates but not in the Landsat based estimates. **(C)** AGB profile 3 (15.2 km long) within a peat swamp forest covering a fire scar from the year 1997 (1.8–10.4 km). The Landsat based AGB estimates are much higher than the LiDAR estimates. Also the LiDAR AGB estimates give an idea on the AGB variability which the Landsat based estimates are not able to give. **(D)** AGB profile 4 (10 km long) within a peat swamp forest covering one fire scars from the year 2002 (2.9–4.1 km) and another fire scar from the year 2006 (7.5–10.0 km). Here also the Landsat based AGB estimates for peat swamp forest are much higher than the LiDAR estimates.

BGD
9, 11815–11842, 2012